Available online at www.sciencedirect.com
SCIENCE DIRECT®
Journal of Sound and Vibration 274 (2004) 323–349
JOURNAL OF SOUND AND VIBRATION
www.elsevier.com/locate/jsvi

Active control of environmental noise, VIII: increasing the response to primary source changes including unpredictable noise ☆

S.E. Wright[a,*], H. Atmoko[a], B. Vuksanovic[b]

[a] *ECASS Technologies Ltd., 22 Moor Lane Laboratories, Highburton, Huddersfield HD8 0QS, UK*
[b] *School of Computing and Technology, University of Derby, Derby DE22 1 GB, UK*

Received 7 August 2002; accepted 20 May 2003

Abstract

Conventional adaptive cancellation systems using traditional transverse finite impulse response (FIR) filters, together with least mean square (LMS) adaptive algorithms, well known in active noise control, are slow to adapt to primary source changes. This makes them inappropriate for cancelling rapidly changing noise, including unpredictable noise such as speech and music. Secondly, the cancelling structures require considerable computational processing effort to adapt to primary source and plant changes, particularly for multi-channel systems. This paper describes methods to increase the adaptive speed to primary source changes in large enclosed spaces and outdoor environments.

A method is described that increases the response to time varying periodic noise using traditional transverse FIR filters. Here a multi-passband filter, with individual variable adaptive step sizes for each passband is automatically adjusted according to the signal level in each band. This creates a similar adaptive response for all frequencies within the total pass-band, irrespective of amplitude, minimizing the signal distortion and increasing the combined adaptive speed.

Unfortunately, there is a limit to the adaptive speed using the above method as classical transverse FIR filters have a finite adaptive speed given by the stability band zero bandwidth. For rapidly changing periodic noise and unpredictable non-stationary noise, a rapid to instantaneous response is required. In this case the on-line adaptive FIR filters are dispensed with and replaced by a time domain solution that gives virtually instantaneous cancellation response (infinite adaptive speed) to primary source changes, and is computationally efficient.

☆ This paper is an extended version of a conference paper given at Active 2002 ISVR Southampton University July 2002.

*Corresponding author.
E-mail addresses: selwyn.wright@ntlworld.com (S.E. Wright), b.vuksanovic@derby.ac.uk (B. Vuksanovic).

0022-460X/$ - see front matter © 2003 Elsevier Ltd. All rights reserved.
doi:10.1016/j.jsv.2003.05.017

1. Introduction

The practical era of active noise control (ANC) system development was hailed in mainly through using transverse finite impulse response (FIR) filters. The period started around 1975 with a single frequency 2 tap notch FIR filter, developed by Widrow et al. [1], and its subsequent extension to multi-tap FIR filters by Glover [2]. Later Morgan [3] and Widrow et al. [4] included the effect of the implementing plant, through the development of the filtered x least mean squared (FXLMS) algorithm. These two basic innovations, the use of FIR filters to cancel the primary source signal and adapt to its changes and the FXLMS algorithm to take account of the implementing plant and adapt to its changes, were the corner stones of modern ANC system development.

Later, Chaplin and Smith [5] described the cancellation of periodic noise through the use of synthesized sound and Elliott and Darlington [6] considered the reduction of periodic noise using a periodic pulse train. Subsequently, Elliott and Nelson [7] investigated the effect of the implementing plant for the cancellation of single frequency sound and Darlington and Elliott [8] included the effect of the plant for periodic noise. Elliott et al. [9] then developed and implemented a multi-channel (multi-secondary sources, multi-error detectors) FXLMS system for the reduction of discrete frequency noise within confined spaces. Finally, Wright and Vuksanovic [10,11] and Wright and Atmoko [12,13] developed and implemented directional ANC systems for the reduction of sound in unrestricted space.

2. Limitations of FIR filters

Most of the above researchers have used transverse FIR filters to cancel both predictable and statistically stationary unpredictable noise, such as broadband noise. If the reference signal from the primary source to be cancelled is non-varying narrow band, then the taps (coefficients or weights) of the FIR filter, after convergence, will represent a cancelling notch filter. If the reference signal is unpredictable statistically stationary broadband noise, then the weights of the filter will converge eventually, providing there are sufficient taps and time. If the reference signal is unpredictable non-stationary noise, then the FIR filter, with a practical number of taps, will not effectively converge, as it will have to adapt continually. Convergence takes a finite time, depending on the complexity and variability of the primary source and plant, and on the number of FIR filter taps.

Preliminary investigations confirmed that

(i) FIR filters adapt with increasing speed (reduced time constant), in cancelling unwanted primary noise, as the number of control taps in the filter is increased.
(ii) There is an optimum number of taps, depending on the complexity of the primary source and complexity of the plant, starting with 2 taps for a single frequency.
(iii) The adaptive speed increases with the cancelling strength $\beta = \mu A^2$, where μ is the adaptive step size of the cancellation noise and A is the peak signal amplitude of the primary source.
(iv) The adaptive speed decreases with increases in the primary source spectrum density, for a given tap number.

This indicates that for a primary source with frequencies of various amplitudes, the adaptive speed reduces as the number of source frequencies increases, with the lower amplitudes adapting more slowly. If the signal is non-varying, then the lower amplitude frequencies will adapt eventually, given sufficient taps and time. But for source frequencies varying in time the smaller amplitudes will not have time to catch up (adapt completely), producing slow adaptation and signal distortion.

However, the adaptive speed of these filters to primary source changes can be increased. The approach is to divide the source spectrum into frequency passbands. Each passband has a separate FIR filter with a similar cancelling strength β, but a different adaptive step size μ_k. This is adjusted to be inversely proportional to the peak signal amplitude squared in each frequency band, i.e., $1/A_k^2$. In this way a similar response, irrespective of frequency amplitude, will then be obtained across the total spectrum. The larger the number of passbands the smaller the frequency band width, the higher the frequency resolution and the more uniform the frequency response.

This multi-passband, variable μ, fixed β method to increase the adaptive speed should not be confused with the normalized LMS algorithm that uses an adaptive step size according to the total reference signal power. The present scheme is illustrated in Fig. 1. The reference signal 'x' from the primary microphone feeds a set of passbands and their individual transverse FIR filters. The output from each filter drives the secondary cancelling speaker. The output E from the error microphone is used to adjust each individual FIR filter over its particular passband, which in turn adjusts the output from the speaker over these same passband frequencies to drive the signal at the error microphone to zero, i.e., making $E \rightarrow 0$ for each passband contribution.

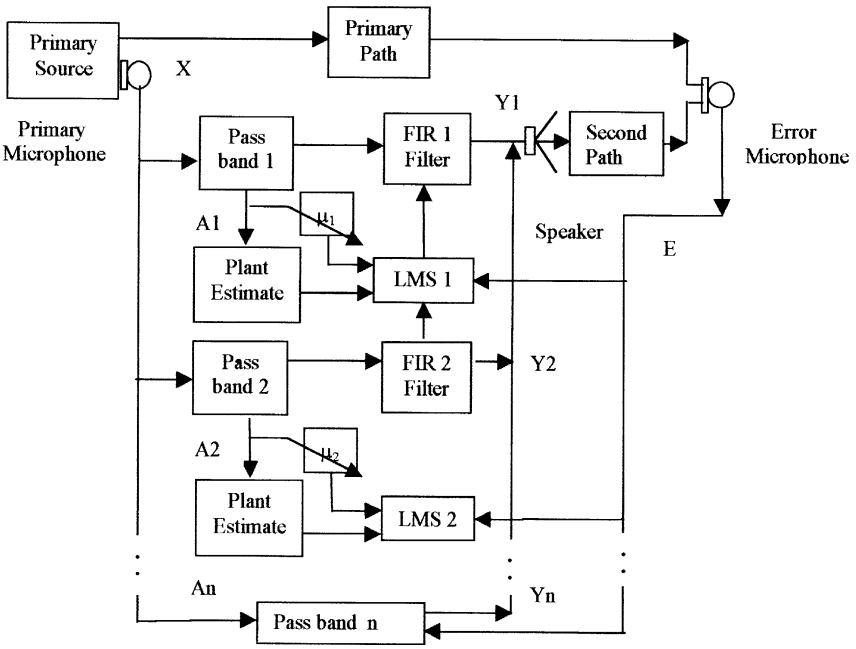

Fig. 1. Multi-passband variable adaptive step size transverse FIR filter.

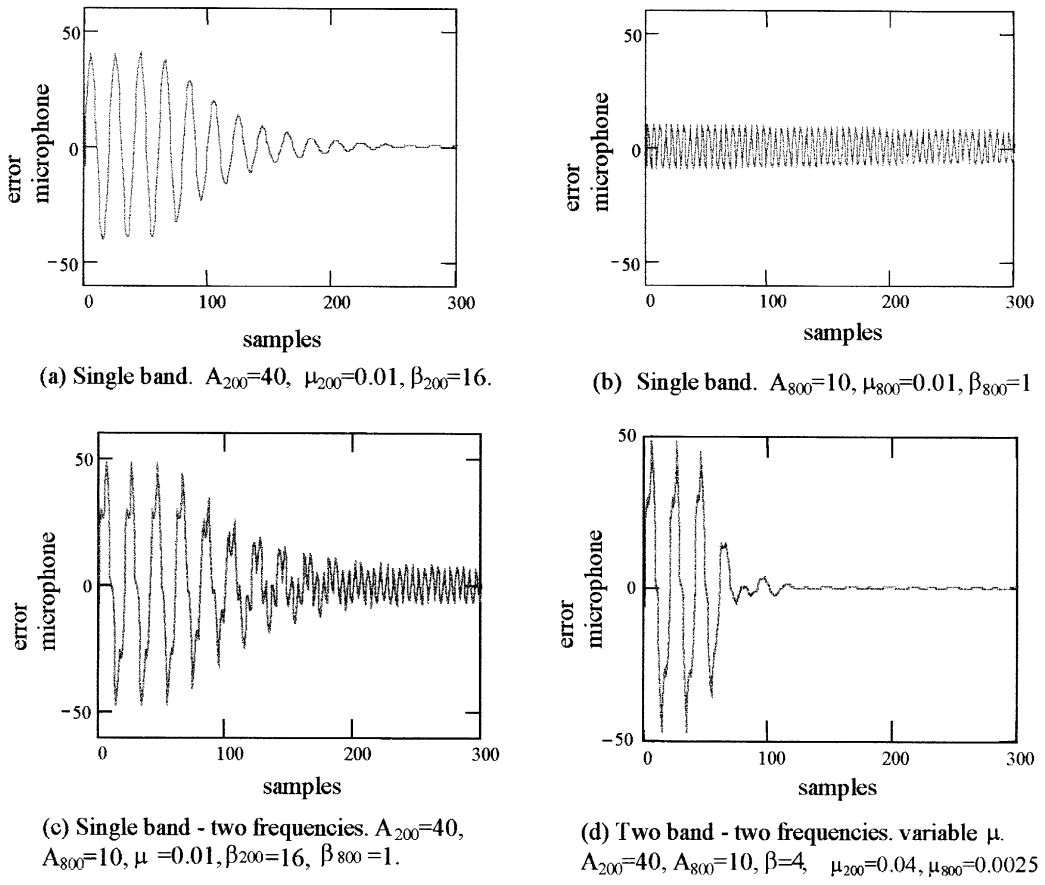

Fig. 2. Single and two-passband FIR filters, with the cancellation of one and two primary frequencies. Sampling frequency $f_n = 4\,\text{kHz}$ and number of weights $w_{fil} = w_{can} = 20$.

Fig. 2 shows the simulations for a single and a two-passband system for a simple second order plant. The adaptive filters and the passband filters each have 20 taps and a sampling frequency of 4 kHz. Fig. 2(a) (signal frequency 200 Hz, amplitude 40 units) and Fig. 2(b) (signal frequency 800 Hz, amplitude 10 units) are computed separately in a single passband with the same step size $\mu = 0.01$, giving $\beta = 16$ and 1, respectively. It can be seen that the lower amplitude (lower β), adapts much more slowly. Fig. 2(c) shows the adaptation with both frequencies now in the same passband, again the lower amplitude signal adapts much more slowly.

Finally, Fig. 2(d) shows the same two frequencies computed together, but each in a separate passband, each having a different μ but now having the same β. The low and high frequency passband cross over is 500 Hz. Both the passband and cancellation filters are represented by FIR filters, each having 20 taps. The figure is computed for maximum adaptive speed, without instability, giving an almost immediate cancellation for both frequencies. The corresponding adaptive step values in each band to give a maximum adaptive speed of $\beta = 4$ is $\mu_{200} = 0.04$ and $\mu_{800} = 0.0025$.

This approach certainly increases the overall adaptive speed of transverse FIR filters considerably, but unfortunately the adaptive speed is limited by a finite β. As β increases the stability bandwidth shrinks until it reaches zero bandwidth [12], this determines its maximum β value. The approach is adequate for many applications, but mainly restricted to changing primary sources such as unsteady periodic noise. Its disadvantage is intensive computation, requiring adaptive passband and cancellation FIR filters for each band. Although the pass band filters could be implemented into hardware reducing the computation burden.

3. Instantaneous cancellation

In summary, it can be said that classical transverse adaptive FIR filters converge at various speeds, depending on the number of filter taps, the complexity of the plant and the primary signal to be cancelled. These filters converge to some form of the inverse of the plant, depending on the spectrum content of primary reference signal. As the reference signal changes, a finite length FIR filter has to readapt, accordingly, in a finite time.

Thus to implement a really fast response to source changes, including unpredictable, statistically non-stationary noise, it is essential to dispense with the on line adaptive FIR filter. A time domain solution that gives virtually instantaneous cancellation response (infinite adaptive speed) to primary source changes, and is computationally efficient, is to use an instantaneous, plant inverse, negative direct replica (IPINDR) approach. Here a negative copy of the primary source signal is used directly to cancel the sound, compensated for plant distortion by passing the signal through the plant inverse, aligned at the instantaneity point (position where the secondary wave is exactly aligned with the primary wave) and matched in amplitude before combining with the primary wave.

3.1. Salient characteristics

(i) The cancelling system has no on line adaptive transverse FIR filters. Apart from convolution, there are no computational demanding processes. An initial, of line, phase and amplitude adjustment is affected, based on a minimum error signal, using a simple sample delay buffer n_b and amplitude regulator A.

(ii) The approach is basically instantaneous to the response of primary source changes, as a negative copy of the primary source signal is passed directly through the secondary source system to the cancelling loud speaker. Although there is delay in the cancelling system, the instantaneousness is preserved by moving back and forth in time along the wave and injecting the cancelling signal at the appropriate instantaneity point.

(iii) The critical alignment in the cancellation process is dependent on the small control distance between the primary microphone and secondary source, $r_{ps} = r_{pm} - r_{sm}$, and not on the secondary source–error microphone control distance r_{sm}, as in the case of the conventional FIR process, where r_{pm} is the primary microphone–error microphone distance. Thus, the control distance r_{ps} is considerably smaller than the control distance r_{sm} making the sensitive propagation space much less vulnerable to environmental changes, such as fleeting reflections, than the adaptive FIR method. The two common environmental propagation

distances r_{pm} and r_{sm} are approximately equal, thus environmental changes tend to affect both these propagation paths equally.

(iv) Acoustically, the primary and secondary sources form a phase-controlled dipole PCD, [12], where the phase of the secondary source is adjusted to be out of phase with the primary sound field at the error microphone. The resulting radiated acoustic field directivity (shadow shape) can be made to be tripole like (cardiod), dipole like (figure of eight) and quadrupole like (four-leaf clover), with successive increases in the dipole moment (separation distance between the primary and secondary source r_{ps}).

(v) The PCD, in the IPINDR case, uses the propagation distance r_{ps} for both the primary and secondary waves. This produces exact alignment between the waves, giving maximum shadow at all points along the wave. Whereas in the conventional adaptive FIR system, the propagation distance r_{pm} is used for the primary path and r_{sm} for the secondary path. This produces exact alignment only at the error microphone, giving a slight phase difference at all other points along the wave, the shadow depth deteriorating progressively with distance.

(vi) The cancelling system is inherently stable, i.e., the error microphone is only needed to set up the cancellation process. After the setting up, the cancellation is self-sustaining, without the use of the microphone, accept for momentary adjustment in strong environmental changes.

3.2. Mode of operation

The system is illustrated in Fig. 3 and operates as follows:

1. The secondary cancelling signal is 'copied' from the primary source using a primary sensing transducer (microphone or equivalent), suitably isolated from the secondary source (shielding and/or directional transducers) to prevent feedback between the two.

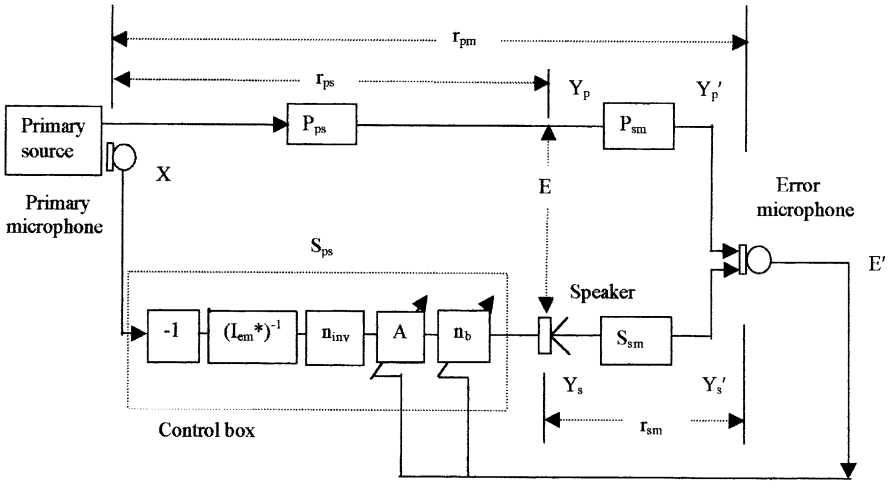

Fig. 3. Instantaneous, plant inverse, negative direct replica (IPINDR) cancelling system. The plant function I_{em} comprises primary microphone, secondary speaker, amplifier and filter transfer functions.

2. The secondary signal is negated in preparation for cancelling the primary signal.
3. The electromechanical plant (impulse) response I_{em}, which produces signal distortion, is neutralized/reduced by one or all of the following:
   (i) physically altering the dynamic response of the dominant component—the sound transducer (loud speaker) and its driver,
   (ii) mathematically modifying the net response of the system through adding the appropriate number of poles or zeros to the overall transfer function,
   (iii) measuring the impulse response of the electromechanical system I_{em}^{*} and inverting the response. The actual I_{em} includes essential components in the secondary sound cancelling path, such as the computer A/D D/A converters, aliasing/quantization filters, amplifiers and loud speakers).
4. The modified plant response, and/ or the inverted response $(I_{em}^{*})^{-1}$, is convolved with the secondary signal, and used to drive the secondary loud speaker.
5. The resulting secondary acoustic wave is combined and aligned with the primary acoustic wave by appropriately positioning the secondary source downstream of the primary source in the direction of the error microphone. This facilitates a time advance along the primary wave represented by the shift function $h_a(t+\tau_a)$. Here the time advance $\tau_a = r_{ps}/c_0$, where τ_a is the propagation time between the primary microphone and secondary source, r_{ps} is the propagation distance between the primary microphone and secondary source and c_0 is the propagation speed (speed of sound). The time advance is necessary to offset the signal retardation represented through the delay function $h_r(t-\tau_r)$, where τ_r is the signal processing time.
6. In terms of samples, generated by a sampling frequency f_n, the time advance $\tau_a = r_{ps}/c_0$, is equivalent to

$$n_a = \tau_a f_n = r_{ps} f_n / c_0. \tag{1}$$

7. The total sample delay n_r is generated through the cancelling system processing delay n_{proc}, which includes the computation delay n_{com}, and the inverse training process delay n_{inv}. Also the adjustable sample delay n_b added, through a delay buffer, to fine-tune the signal alignment offline. Online, environmental changes have little effect on n_b and its value is fixed for all but severe environmental changes. The total retardation sample number becomes

$$n_r = n_{proc} + n_b, \quad n_{proc} = n_{com} + n_{inv}. \tag{2}$$

8. The sample advance n_a is adjusted through the distance between the primary microphone and secondary source r_{ps}. The delay buffer n_b is then adjusted until $n_a = n_r$, giving a minimum error E' at the error microphone.
9. The amplitude A of the secondary signal is adjusted to match that of the primary source signal giving a further minimum error E' at the error microphone.
10. The last two steps are successively repeated until the lowest minimum error E' is achieved. This ensures that the secondary and primary signals are in alignment at the error microphone, and all points along the wave.

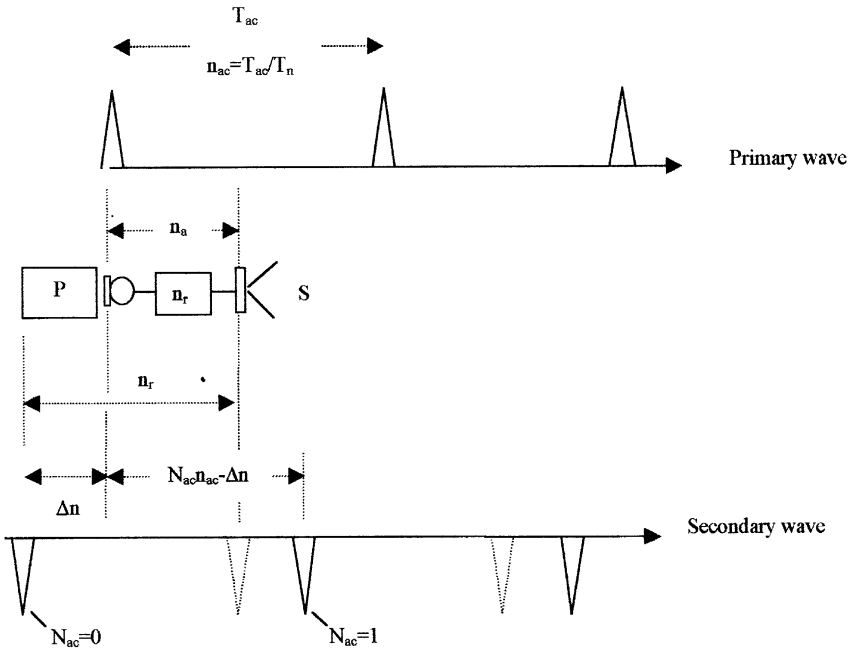

Fig. 4. Secondary wave alignment with primary wave, in sample numbers.

3.3. Mathematical description

For a primary acoustic wave of periodic frequency f_{ac} moving to the right, the secondary wave alignment with the primary wave in samples at the secondary source (loud speaker), is illustrated in Fig. 4. The secondary wave is shown as dotted line pulses as measured at the primary microphone and outputted directly from the loudspeaker, without any delay between the primary microphone and loudspeaker ($n_r = 0$). Moving the speaker to the right by n_a samples of course moves the secondary wave with it and advances its time compared to the primary wave. The full lined pulse is the position of the secondary wave after including a processing delay n_r. Also n_{ac} is the number of samples in the period T_{ac} of the primary wave and T_n is the sampling period. N_{ac} is the period number that the primary wave is in advance of the secondary wave. The relationships are:

$$N_{ac}n_{ac} - \Delta n = 0, \quad \Delta n = n_r - n_a, \quad n_{ac} = T_{ac}/T_n = f_n/f_{ac}. \tag{3}$$

Rearranging Eq. (3) gives

$$n_a = n_r - N_{ac}f_n/f_{ac}. \tag{4}$$

For a slowly changing periodic noise the system can be non-casual, i.e., the delay $n_r(\tau_r)$ can be longer than the advance $n_a(\tau_a)$, here only the periods need to be aligned, i.e., N_{ac} can be any integer. For unpredictable noise the signals must be casual and exactly aligned at the instantaneity point, the advance must balance the delay exactly, i.e., $N_{ac} = 0$ and $n_a = n_r$, making

$$h(t + \tau_a)h(t - \tau_r) = h(t + \tau_a - \tau_r) = h(t). \tag{5}$$

Referring back to Fig. 3, the difference between the primary signal Y'_p and secondary signal Y'_s at the error microphone becomes

$$E'(t) = Y'_p - Y'_s = X(t)*[P_{ps}*P_{sm} - h(\tau_a - \tau_r)*I_{em}*(I^*_{em})^{-1}*S_{ps}*S_{sm}], \tag{6}$$

where $*$ indicates convolution, $X(t)$ is the reference signal at the primary source, P_{ps} and P_{sm} are the primary path responses, i.e., primary to secondary source and secondary source to microphone, respectively. Again $h(\tau_a - \tau_r)$ is the time shift function either advance τ_a through moving the speaker to the right or delay τ_r through the signal processing. I_{em} is the actual electromechanical plant impulse response of the cancelling system and $(I^*_{em})^{-1}$ is the measured or calculated inverse of the electromechanical plant impulse response. S_{ps} and S_{sm} are the primary–secondary source and secondary source–microphone path responses, respectively. It is assumed that the primary microphone has a flat response and unity gain. If the propagation paths $P_{ps} = S_{ps}$ and $P_{sm} = S_{sm}$ and A is an amplitude adjustment, then the difference signal at the secondary loud speaker becomes

$$E(t) = Y_p(t) - Y_s(t) = X(t)*S_{ps}(t)*[1 - A*h(\tau_a - \tau_r)*I_{em}*(I^*_{em})^{-1}]. \tag{7}$$

In the frequency domain Eq. (7) becomes

$$E(f) = Y_p(f) - Y_s(f) = X(f)S_{ps}(f)[1 - Ae^{j2\pi f(\tau_a - \tau_r)}B(f)/B^*(f)e^{j(\theta - \theta^*)}]. \tag{8}$$

For a time varying periodic noise or unpredictable noise, the signals have to be matched at the instantaneity point. Thus the zero order period $N_{ac} = 0$ in Eq. (4) has to be used, giving $n_a = n_r$, $\tau_a = \tau_r$ and $e^{j2\pi f(\tau a - \tau r)} = 1$. B and B^* are the amplitudes and θ and θ^* are the phases of the impulse response I_{em} and estimated (measured) response I^*_{em}, respectively. For zero frequency distortion, the plant dynamics has to be neutralized completely, from Eq. (8)

$$A = B^*/B, \quad \theta^* = \theta \quad \text{giving } E = 0. \tag{9}$$

There is a minimum distance r_{ps} between the primary and secondary source for the cancellation of unpredictable noise to be achieved. This is determined by the secondary path processing time which is basically the delay n_{inv} required in the inverse function realization if the computation delay can be neglected. From Eqs. (1), (2) and (9) this distance is given by

$$r_{ps} = n_{inv}c_0/f_n. \tag{10}$$

This is the threshold distance for the cancellation to succeed. n_{inv} can be large for non-minimum phase plant functions.

3.4. Shadow bending

The phase control dipole shadow can be moved away from its dipole axis by an angle α_B. For a given change in $n_B(\Delta n_a)$ from a line joining the primary and secondary sources, Eq. (1) gives

$$n_B = \Delta(r_{ps}f_n/c_0), \quad \Delta r_{ps} = r_{ps} - r'_{ps} = r_{ps}(1 - \cos\alpha_B), \tag{11}$$

where r'_{ps} is the propagation distance in the direction of the shadow minimum. Rearranging the above equation gives

$$\alpha_B = \cos^{-1}[1 - n_B c_0/f_n r_{ps}]. \tag{12}$$

The shadow bending or rotation from the source axis, per n_B, therefore depends on the relative magnitude $f_n r_{ps}$ compared to c_0. For a given sampling frequency the shadow rotation position can be controlled by altering n_B or r_{ps}. For example $f_n = 16\,\text{kHz}$, $r_{ps} = 0.2\,\text{m}$ and $c_0 = 340\,\text{m/s}$, $\alpha_B = 26^\circ$ per n_B.

3.5. Multi-channel systems

For practical cancelling systems, requiring wide shadows, particularly at high frequencies, multi-channel (multi-speaker/multi-detector microphone) systems are required.

3.5.1. Conditions for cancellation

Generally, for cancellation using free-field multi-channel systems, Huygens principle needs to be understood and implemented. Huygen realized that any continuous source distribution and resulting propagating wave can be represented by a series of point sources each radiating spherical waves. This realization makes it possible to represent and cancel the radiation from an extended primary source (one whose source is continuous and size is larger than its acoustic wavelength), using a finite distribution of (small) point secondary sources, providing they are close enough together (less than half an acoustic wavelength).

Then each spherically propagating wavelet from each region on the primary source, radiating forwards and sideways, will be matched by secondary cancelling sources, where of course a negative replica of the primary source radiation is required. Even for acoustic wavelengths smaller than the primary source distribution, complex acoustic interference from phase path differences from different points on the primary source, will be matched by similar phase path differences from the cancelling secondary sources making practical acoustic shadows possible.

To set up an effective cancelling wave front, the forward and lateral radiation has to be taken into account at each detection microphone in the adaptive algorithm. This is accommodated through the cross-coupling terms in the initial adaptive algorithm. Each secondary cancelling speaker output is adjusted according to the minimum error signals at all the monitoring microphones. The error signals at all microphones are of course a function of all the cancelling speaker outputs. This cross-coupling produces a complex array of outputs from the cancellers and a corresponding complex acoustic field at the error microphone array.

The spatial shadow distribution across the microphone array depends on the secondary source–microphone distances r_{sm}. Generally, the acoustic field has deep minima at individual microphone positions with a higher average spatial field away from the microphones. As the distance r_{sm} increases compared to the primary–secondary source distance r_{ps}, the cancelling field becomes more spherical and coincident with the primary field. This results in the microphone minima reducing and the cancellation field becoming smoother and deeper, satisfying Huygens condition more completely. An extensively cancelled field, almost over an unlimited number of wavelengths, results. This is in contrast to diffuse, reverberant regions within small enclosures where the cancellation region is limited to less than half an acoustic wavelength.

In the case of a single channel IPINDR PCD cancelling system a narrow shadow is produced. For practical systems and as high frequencies, multi-channel (multi-speaker/multi-detector) systems are required to fulfill Huygens description. The primary source microphones, secondary cancelling sources and error microphones are generally arranged in successive planes or arcs from

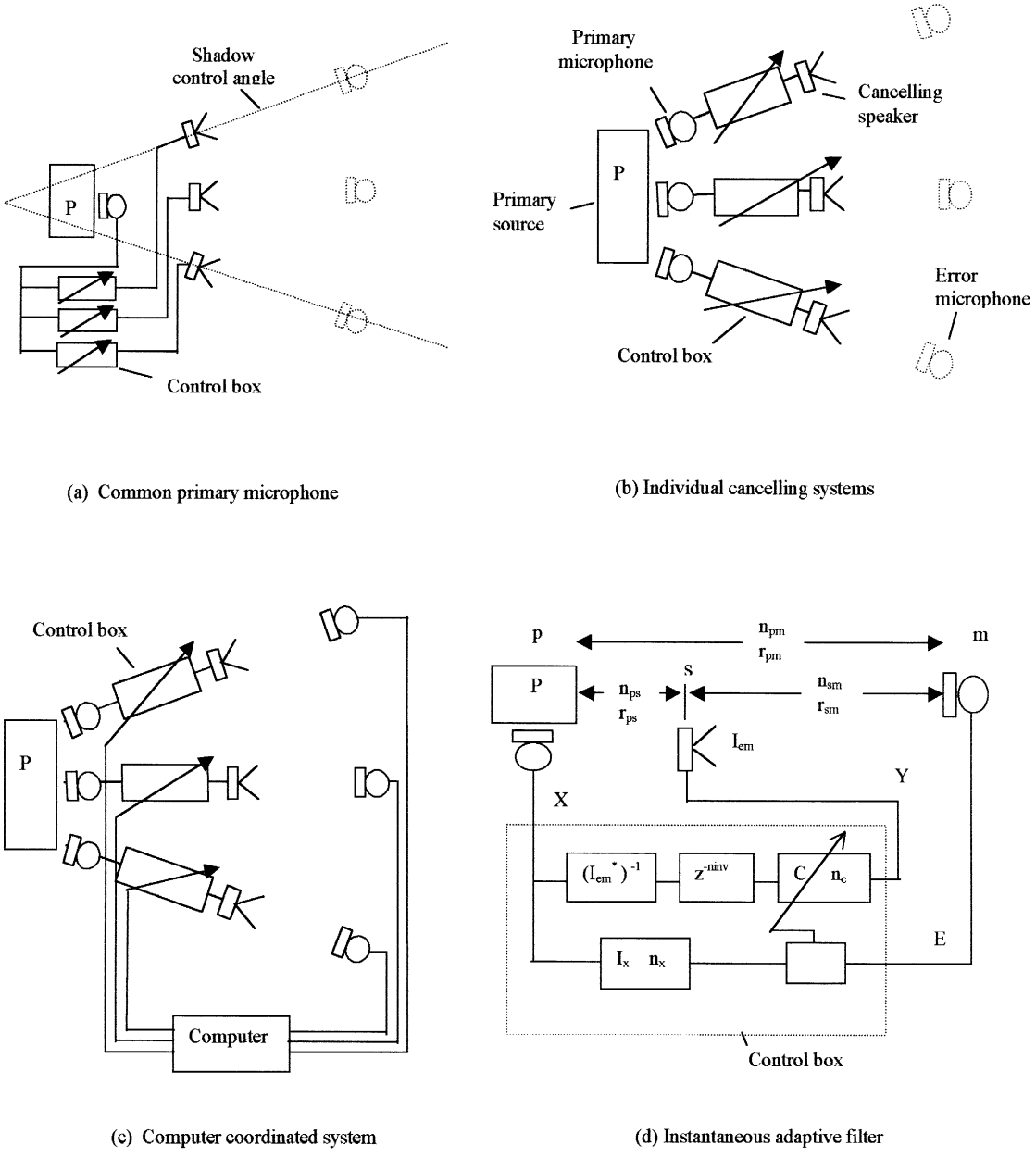

Fig. 5. Multi-channel IPINDR cancelling systems.

the primary source and contained within control angles, both vertically and horizontally, forming the boundaries for well defined acoustic shadows, as illustrated in Fig. 5 and explained in detail in Ref. [13].

Further, for these systems to operate effectively, the acoustic path differences $(\Delta r)_{pd}$ between the various combinations of cancelling speakers and error microphones of multiples (p) of

acoustic half wavelengths ($\lambda_p = c_0/f_p$, where f_p is a series of frequency peaks) should be avoided. These path differences correspond to a series of maxima in the maximum to minimum eigenvalue ratio in the propagation matrix characteristic equation, as described further in Ref. [13]. This gives the following condition:

$$(\Delta r)_{pd} = pc_0/2f_p, \quad \text{where } p = 1, 2, 3, \ldots, \text{etc.} \tag{13}$$

Or in terms of sample numbers, for a discrete sampling system, $n_{pd} = \tau f_n$ where $\tau = (\Delta r)_{pd}/c_0$, the uncontrollable sample numbers and uncontrollable frequencies to be avoided become

$$n_{pd} = pf_n/2f_p \quad \text{or} \quad f_p = pf_n/2n_{pd}. \tag{14}$$

These multi-channel systems are fundamentally stable in that they do not require the error microphone to maintain cancelling stability. The cancelling system is basically instantaneous to the response of primary source changes, as a negative copy of the primary source signal is passed directly through the secondary source system to the cancelling loudspeaker. Apart from convolution, there are no computational demanding processes either. A simple phase and amplitude error adjustment is affected using a delay buffer and amplitude regulator. All configurations are capable of shadow angle rotation through appropriate adjustment of n_B, r_{ps} or f_n.

3.5.2. Practical configurations

For a non-changing plant the error microphone can be dispensed with after the initial setting up to produce minimum error (sound). Thus each channel can be set up independently, requiring no inter-channel co-ordination. Fig. 5(a) shows the configuration for a small or large in-phase primary source. Here a single primary microphone is sufficient to drive all the secondary sources. A single error microphone is sufficient to adjust each channel, one at a time, at each of the angle positions, as indicated with the dotted outline. With in the adjustable control boxes are the control elements shown in the chain dotted box in Fig. 3.

Fig. 5(b) is a configuration for an out of phase primary source (for example modal distributions within a metal structure). Here separate primary microphones are used to measure the local sound across the primary source and drive each channel separately, making them self-contained units. Each unit consists of a primary microphone, control box and loudspeaker. Again only a single error microphone is used in turn, at each angular position, to minimize the error signal for each channel, one at a time, with repeated passes over each microphone until the averaged minimum shadow is achieved.

Of course a multi-channel computer co-ordinated system should always out-perform a set of independent channels. A computer co-ordinated multi-channel system is shown in Fig. 5(c) for off-line adjustment or momentary on line adjustment for severe environmental changes. An array of cancelling units and an array of permanent error microphones, in full line, is shown. Each of the error microphones and control boxes are linked to a computer. The amplitude A and delay n_b adjustment elements in the control boxes can be co-ordinated through the computer to align channels to give a collective minimum error at the error sensors.

These control elements can also be replaced with, for example, a simple C filter (few taps transverse FIR filter and a modified filtered x algorithm). The last figure, Fig. 5(d), illustrates such an adjustment scheme, where n_{ps}, n_{sm}, and n_{pm} are propagation distances in sample numbers

between the primary and secondary sources, secondary source and error microphone and primary source and error microphone, respectively. The relationships between these propagating distances in samples and the secondary plant impulse response I_{sm} are

$$n_{ps} + n_{sm} = n_{pm} \quad \text{and} \quad I_{sm} = I_{em} z^{-nsm}, \tag{15}$$

where z is the z domain discrete time transform. Now the inverse of the electro-mechanical plant $(I_{em})^{-1}$ tends to be an unrealizable advanced (negative time) non-minimum phase function. To use these advanced functions in the real world a delay n_{inv} is needed to move them to the right into positive time. This can be achieved, for example, through training a FIR filter and plant in parallel with the appropriate delay off line, as explained in Section 3.6.1. After training, the filter weights represent the realizable delayed function $(I_{em}^{D})^{-1} = (I_{em}^{*})^{-1} z^{-ninv}$. This delayed function is used in the control box together with the C filter and the modified filter x. The accompanying filtered x impulse response I_x and C filter delay value n_c then become

$$I_x = (I_{em}^{D})^{-1} I_{sm} = (I_{em}^{*})^{-1} z^{-ninv} I_{sm} = (I_{em}^{*})^{-1} I_{em} z^{-(nsm+ninv)}. \tag{16}$$

If $I_{em}^{*} = I_{em}$:

$$I_x = z^{-(nx)}, \quad n_x = n_{sm} + n_{inv} \quad \text{and} \quad n_c = n_{pm} - n_x = n_{pm} - n_{sm} - n_{inv} = n_{ps} - n_{inv}. \tag{17}$$

This adjustment scheme is practically instantaneous. If the control system inverse is an accurate estimate, i.e., $I_{em}^{*} = I_{em}$, then the filtered x delay n_x becomes simply the sum of the secondary path delay n_{sm} and the inverse delay n_{inv} and the C filter delay n_c then becomes the difference between the primary secondary source delay n_{ps} and the inverse delay n_{inv}. For unpredictable noise $n_c > 0$, i.e., n_{ps} must be greater than n_{inv}. Here the c filter can act as a delay making up the difference between $n_{ps} - n_{inv}$. For predictable noise n_c can be less than zero allowing $n_{ps} < n_{inv}$. Here, the filter appears to act as an advance device making up the difference between $n_{inv} - n_{ps}$ to reduce the minimum distance r_{ps} in Eq. (10). This is possible because the future and past are identical for predictable noise.

3.6. Inverse functions

To obtain minimum distortion of the secondary cancelling signal (maximum cancellation of the primary wave), it has been shown that an important part of the cancellation process is to obtain a neutralization of the plant transfer function. This can be obtained through an accurate inverse impulse response estimate of the electro-mechanical plant $(I_{em}^{*})^{-1}$ and convolving it with the actual plant function I_{em}, as already discussed.

There are problems obtaining estimates of inverse plant functions, as inverted functions are potentially unstable. For example proper functions (functions with more poles than zeros) become improper functions having more zeros than poles when inverted. Or even more seriously, functions with 'unstable' zeros lying outside of the unit circle in the Z domain become unstable poles (non-minimum phase functions) when inverted. These functions have exponentially decaying negative time (advanced) sequences to the left of time zero, making them difficult to realize. After inversion zeros lying inside the unit circle have exponentially decreasing positive time (delayed) sequences to the right of time zero. Zeros lying on the unit circle have both positive and negative time sequences. Zeros lying near to the centre of the unit circle or at large distances

outside the unit circle have a weak influence on the system, resulting in short time sequences. One can anticipate that when dealing with inverse functions curious properties can result in this upside down world of bringing the future into the past.

3.6.1. Previous investigations

Early investigations using plant inverse functions were in the area of room acoustics. Here the response of a reverberant room distorts the direct sound path between the source (speaker) and receiver (microphone) through reflections around the room. These reflections, if the walls are hard enough ($>40\%$ reflecting), can set up standing waves (resonance's) that can produce zeros (minima) in the acoustic transfer functions. The result, for example, is the speaking into a beer can effect in the early speaker-phones.

Neely and Allen [14] realized the acoustics problem involved and its solution. They neutralized the acoustics plant by passing the signal through the plant (room acoustic response) inverse. The investigators reduced the room distortion through inverting the room response, which fortunately happened to be a minimum phase function. Miyoshi and Kaneda [15] introduced further improvements by dealing with non-minimum phase functions. The approach here was that even if the room had echoes (resonances in the room transfer function, resulting in zeros), the resulting non-minimum phase inverse functions and room distortion effect could be minimized. This was achieved through having either multi-speakers and/or multi-microphones, avoiding, filling in or averaging out the sound zeros in each of the acoustic transmission paths between the speakers and microphones.

Kaelin and von Grunigen [16], in the area of ANC, successfully used a plant inverse to improve the ANC performance and reduce the computational burden of a classical transverse adaptive FIR filter. Using prior off-line measurements of the plant inverse, the controller was split into a long fixed filter part (500 taps) for the reduction of statistically stationary broadband noise reduction and a short adaptive part (30 taps) for the reduction of discrete noise. Significant suppression of the sound in a 5 m long duct, using a single channel, was achieved. These researchers did not consider the problems of non-minimum phase functions directly or an appropriate filtered x adaptive algorithm. Because of the large number of on-line taps, the controller could only respond slowly to changing primary sources.

3.6.2. Time domain inversion

Inverted functions can be obtained in the time domain through measuring an estimate of the plant inverse response $(I_{em}^*)^{-1}$ directly in series with the actual plant I_{em}. This is accomplished off line, using a white noise training signal, as illustrated in Fig. 6(a). The training signal is passed successively through the plant transfer function to be inverted and a FIR filter, using a least mean square (LMS) adaptive algorithm. Band limited white noise or a periodic pulse generator can be used in the training process. The FIR filter adapts to produce a minimum error $E[n]$ at the FIR output summation point resulting in the plant inverse response $(I_{em}^*)^{-1}$.

For advanced negative left handed sequences, (non-minimum phase functions), it is necessary to use 'n_{inv}' samples training delay, in parallel with the plant and FIR filter. This delays the sequence to the right of time zero, converting the unrealizable advanced function into a useable delayed function. The delay is inert, dynamically, apart from retarding the function. The delay allows the training process to converge, where the training error reduces from infinity to near zero,

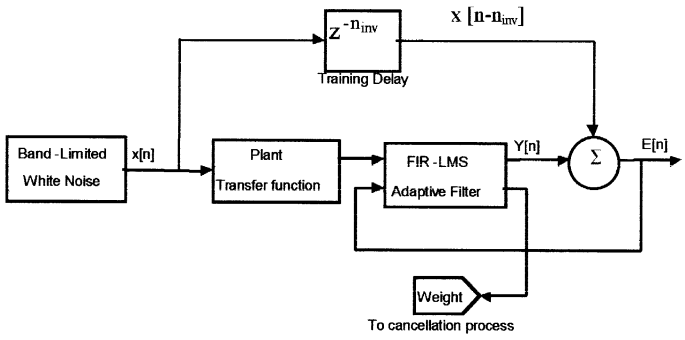

(a) Time domain plant inverse

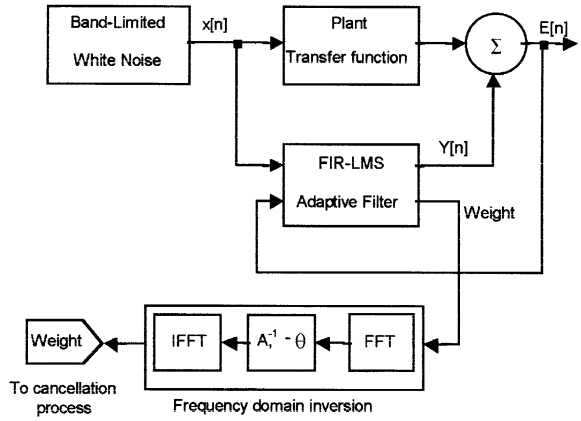

(b) Spectrum domain plant inverse.

Fig. 6. Schematic diagrams showing schemes to obtain the plant inverses.

as the sequence is moved from the future (advanced negative left) to the past (delayed positive right). Unfortunately, these convergence delays become part of the computational processing delay. As a rule of thumb, the number of samples delay needed to invert a function was originally estimated to be approximately half the impulse response length in samples according to Widrow and Stearns [17]. It is now known that the delay can be anything from zero to a large value, depending on the function to be inverted. Minimum phase functions (primarily functions not having 'unstable' zeros) have very short inverted sequences to the right of time zero.

Fig. 7 shows some common transfer functions, their impulse responses and their inverses using a 32 tap FIR filter and 4 kHz sampling frequency. Figs. 7(a)–(c) show typical first, second and third order system responses, respectively. These inverses converge without any delay. There is a one, two and three samples delay shift to the right, in the impulse responses, as the denominator order increases. The resulting inverses which are displayed on the right-hand side of the impulse

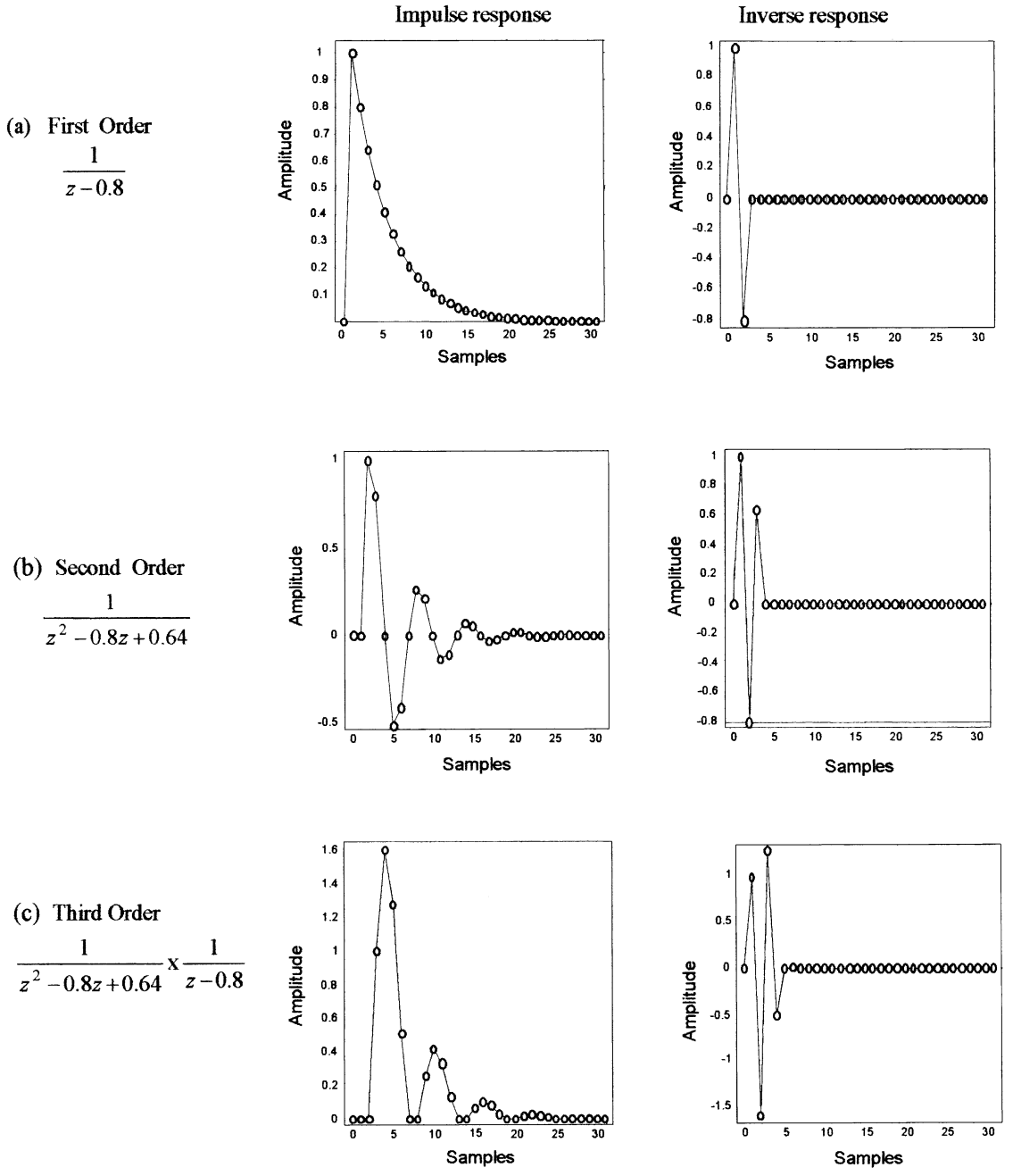

Fig. 7. Some well-known transfer functions, their impulse and inverse responses $w = 32$, $f_n = 4\,\text{kHz}$.

response are much shorter than their corresponding impulse responses. The inverses have to be short and sharp if they are to neutralize abruptly the slowly decaying inertial impulse responses.

Basically a non-zero value sample extension is added for each increase in order, making the overall inverse length 2, 3 and 4 samples, respectively. For example, the second order system used

($z^2 - 0.8z + 0.64$) has a polar radius of 0.8 and a polar angle of 60° (resonant frequency 667 Hz). The first leg amplitude of the inverted function is unity, the middle leg is −0.8 and the third leg 0.6. Increased frequency (increased polar angle) decreases the amplitude of the middle leg. Increased damping (decreased polar radius) decreases the amplitude of the middle and third leg of the inverse function (not shown).

Fig. 8 shows the effect of adding a zero to the second order transfer function. Here the figure is computed using a parallel delay of $n_{inv} = 16$, shifting the inverses from left to right by 14 samples. Fig. 8(a) shows the effect of adding a 'stable' zero, lying inside the unit circle, to the second order system. Its main effect is to produce an exponentially decreasing response to the right-hand side of the inverted function. Fig. 8(b) shows the effect of adding a 'marginally stable' zero lying on the unit circle. This is the worst-case situation and should be avoided. Here the inverse has both large left and right handed sequences and a positive to a negative dc level shift as the zero moves from inside to outside of the unit circle (not shown). Fig. 8(c) shows the effect of adding an 'unstable' zero lying outside the unit circle. Its effect is now to add an exponentially decreasing response to the left side of the inverted response.

It can be seen that the realizable positively delayed sequences, beyond the right of time zero, require no delay. However, the unrealizable negative advanced sequences, to the left of time zero, need added delay to move them from the negative left to the positive right, to bring them into the real world. These large negative sequences require large delays to realize them, impacting the processing time. For small processing delays the negative sequences need to be as short as possible.

3.6.3. Frequency domain inversion

A method that is inherently stable, which is guaranteed to obtain inverse non-minimum phase functions, without the use of an initial delay, is to derive the inverse from the impulse response. Fig. 6(b) illustrates the spectrum domain alternative scheme of obtaining the inverse. Here the plant transfer function is obtained through an adaptive FIR filter in parallel with the plant using a white noise training signal. The transfer function in terms of FIR taps (weights or coefficients) is then frequency transformed, using fast Fourier transform (FFT), to obtain amplitude and phase components. The inverse is then obtained through reciprocating the amplitude and negating the phase. These components are then transformed back into the time domain in terms of FIR filter taps, using inverse FFT (IFFT).

Mathematically, the FFT or swept spectrum or equivalent on I^*_{em} becomes

$$\mathrm{FFT}(I^*_{em}) = \sum (B\,\mathrm{e}^{\mathrm{j}w\theta}), \tag{18}$$

where the spectrum amplitude and phase are B and θ, respectively and $\sum$ indicates summation over all frequencies. The inverse is then obtained by simply inverting B and negating θ, and reassembling the time history again, thus

$$\mathrm{IFFT}\sum (B\,\mathrm{e}^{\mathrm{j}w\theta}) = \sum (B^{-1}\mathrm{e}^{-\mathrm{j}w\theta}) = (I^*_{em})^{-1}. \tag{19}$$

Fig. 9 shows the same plant transfer functions as in Fig. (8), but with their frequency domain transforms of amplitude and phase computed. The frequency inverse is obtained by a simple inversion and negation, respectively. Reverting back to the time domain these frequency inverses reconstruct the time domain inverses but appear split at each end of the FIR filter response. The

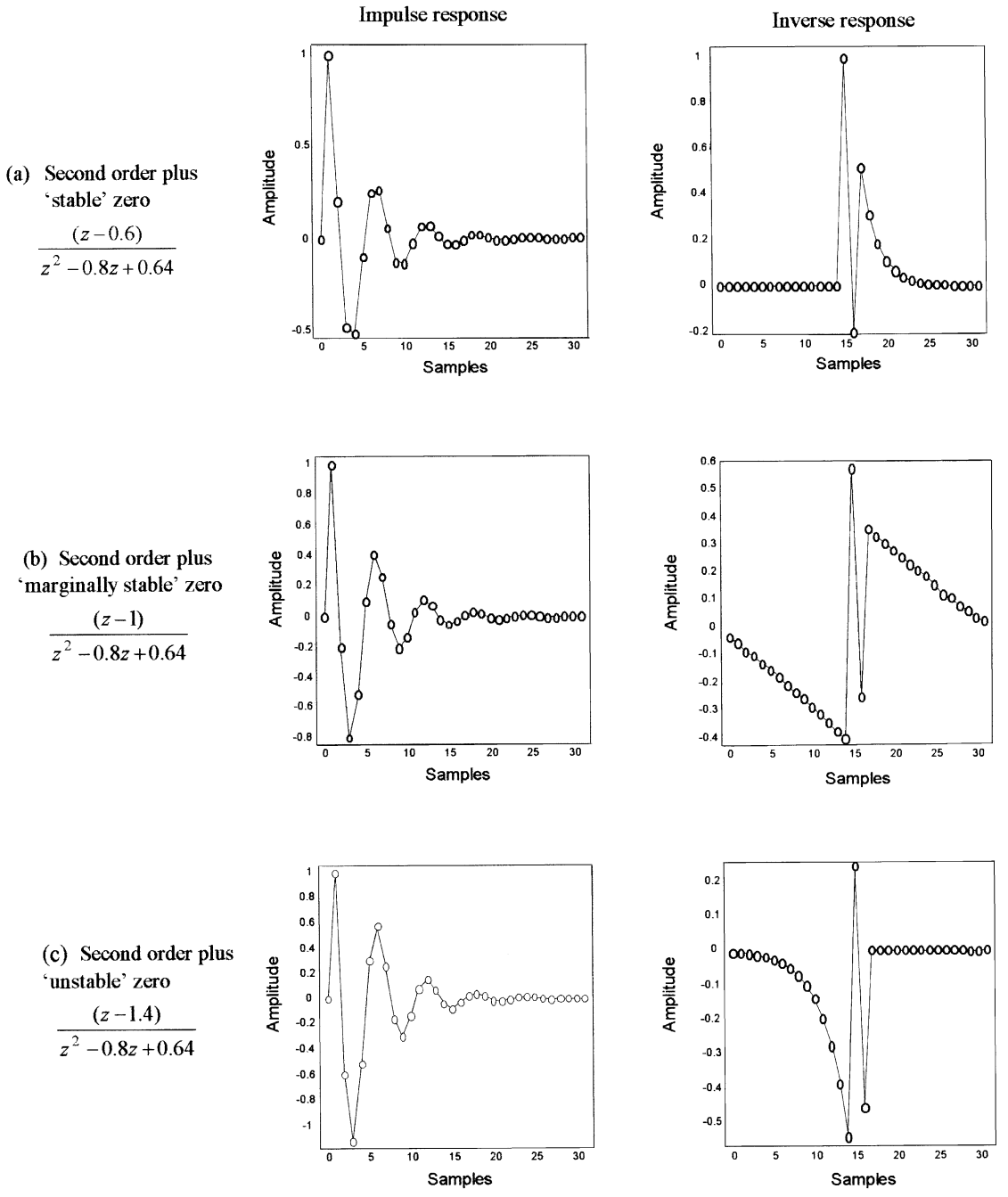

Fig. 8. Second order systems with stable, marginally stable and 'unstable zeros, their impulse and their inverse responses. $w = 32$, $n_{inv} = 16$, $f_n = 4\,\text{kHz}$.

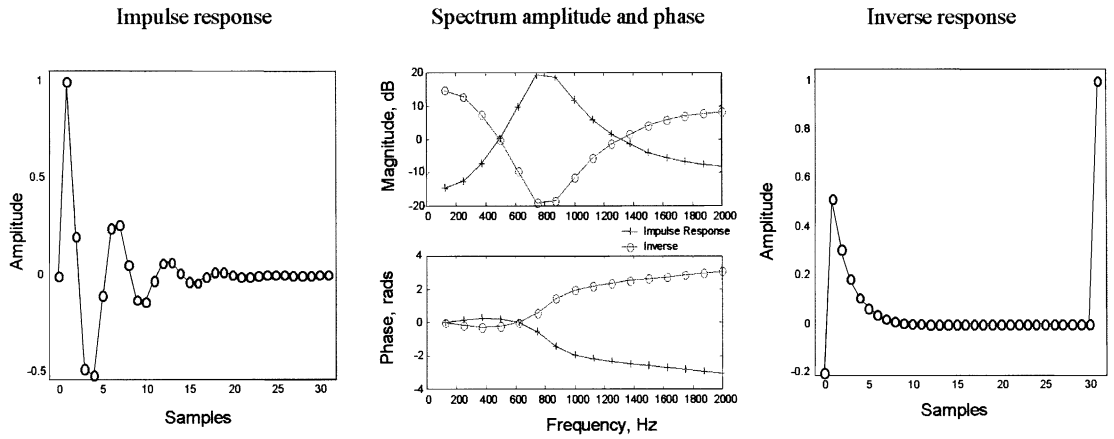

(a) Second order 'stable' zero, $(z-0.6)/(z^2-0.8z+0.64)$.

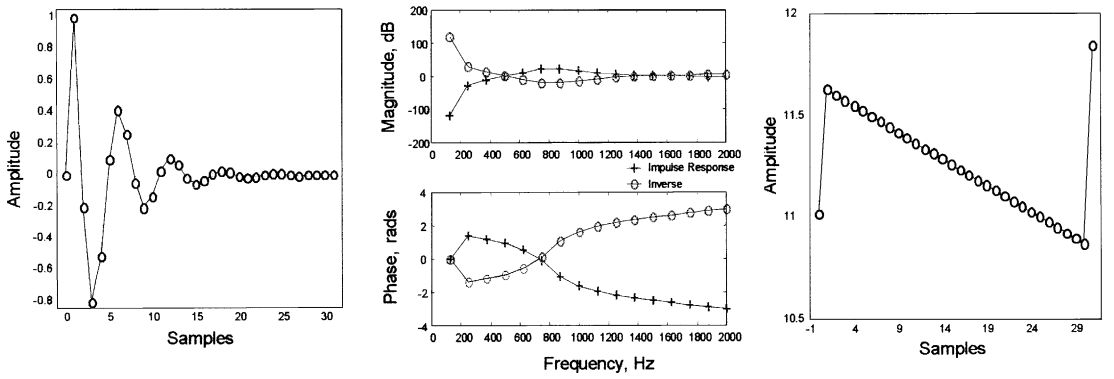

(b) Second order 'marginally stable' zero, $(z-1.0)/(z^2-0.8z+0.64)$.

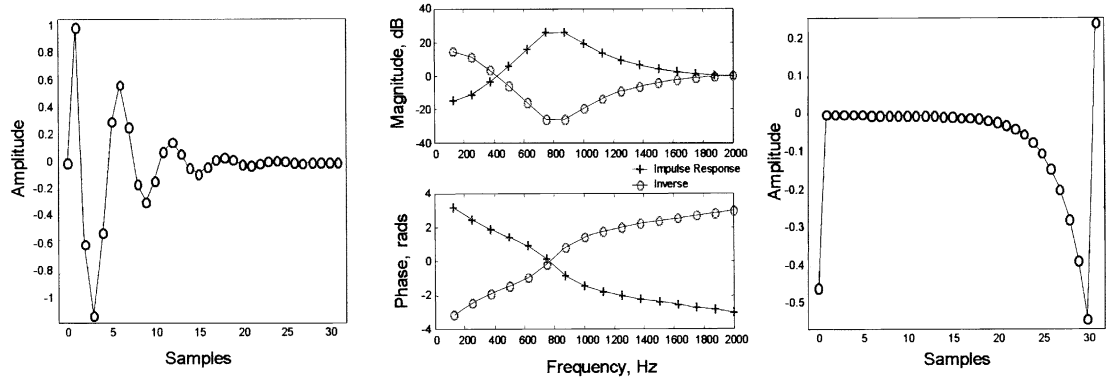

(c) Second order 'unstable' zero, $(z-1.4)/(z^2-0.8z+0.64)$.

Fig. 9. Second order system inverses assembled through the frequency domain.

splits can be moved and assembled anywhere in the filter coefficients, to the right using an advance, or to the left using a delay.

3.7. Cancellation results

Before actual on line cancellation is considered simulation of the cancellation process is computed.

3.7.1. Cancellation simulation

The resulting tap values representing the delayed inverted function $(I_{em}^{D})^{-1} = (I_{em}^{*})^{-1} z^{-ninv}$, from the training process in Fig. 6, are transferred to the simulated cancelling system. Either band limited white noise or a periodic pulse train can be used for the primary reference signal $X(n)$. The primary signal is then convolved with the delayed inverted function and the convolution result passed through the actual plant transfer function I_{em}. The signal is then negated, amplitude adjusted and delayed to produce the secondary cancelling signal $S(n)$. Finally, the secondary signal $S(n)$ is added to the primary signal $P(n)$ to produce the cancelled error signal $E(n)$. The actual simulated cancelling system complete with input and output facilities is illustrated in Fig. 10.

Fig. 11 gives simulated cancellation signals for a simple second order plant $(z^2 - 0.8z + 0.64)^{-1}$ whose response and inverse response is shown in Fig. 7(b). The plant is driven by a 5% duty cycle pulse train primary signal with a pulse repetition frequency of 100 Hz. Figs. 11(a) and (b) show the plant response and the trained inverse plant response to the primary signal. Fig. 11(c) shows the difference between the direct primary signal and its neutralized plant secondary signal showing a very small cancellation signal error of −60dB (one thousandth of the primary signal).

Fig. 12 shows the simulated cancellation for a non-minimum phase plant (the same second order plant as in Fig. 11 but with an additional 'unstable' zero whose response properties are as depicted in Fig. 8(c). The system has a delay of 16 samples and is driven by the same primary pulse train signal. The inverse response is now much wider on its left-hand side, as predicted. However,

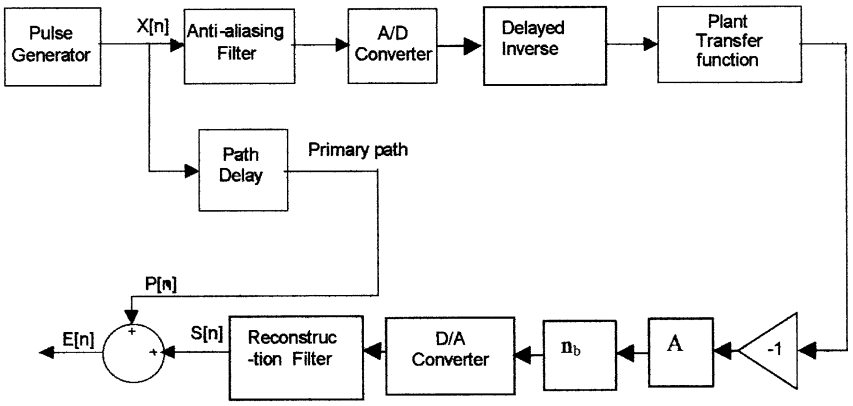

Fig. 10. Plant simulation of cancelling system illustrated in Fig. 3.

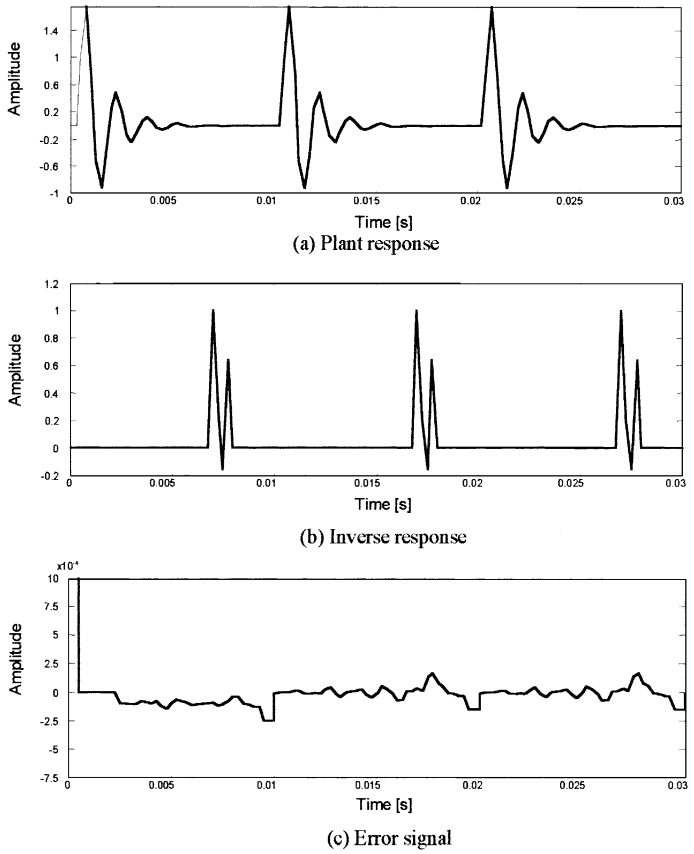

Fig. 11. Cancellation using second order plant using 100 Hz periodic pulse train, 5% duty cycle, $f_n = 4$ kHz.

there is still no problem using non-minimum phase plants, the cancellation has a similar low error between the primary and secondary signal.

Fig. 13 shows the same configuration as in Fig. 12 but replacing the periodic noise with broadband primary noise with a limiting upper cut-off frequency of 800 Hz. The error signal here is now about 3% (−30dB) of the original primary signal. The above simulations show, in principle, that the IPIDNR technique, for cancelling both predictable and unpredictable noise is viable.

3.7.2. Cancellation online

For optimum cancellation and minimum environmental influence on the cancellation process, the primary microphone–secondary speaker propagation advance time τ_a (determined by the distance r_{ps}) needs to be as small as possible. On the other hand this propagation time has to be large enough to offset the secondary path time delay τ_r. This time delay is dominated by the training delay n_{inv} required to obtain the inverse of the plant response. The system response, in these laboratories measurements, is dominated by the secondary loudspeaker-power amplifier dynamics. Measurements, using white noise impulse techniques and a periodic pulse train, showed

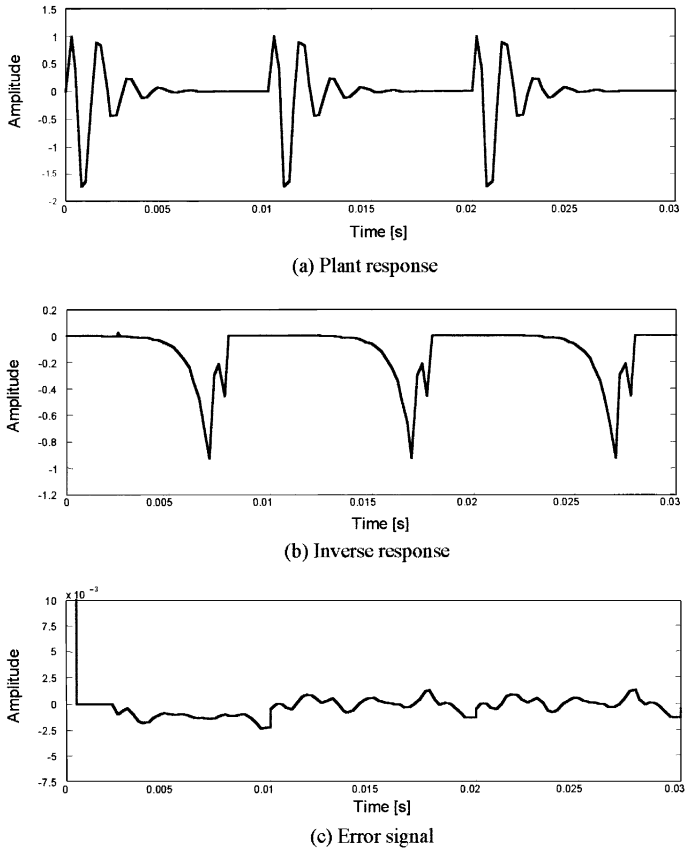

Fig. 12. Cancellation using non-minimum phase plant using 100 Hz periodic pulse train, 5% duty cycle $f_n = 4$ kHz.

the speaker response to comprise of a basic speaker suspension resonance of approximately 200 Hz and a speaker diaphragm-electrical resonance of 2 kHz.

The impulse response, used in the on-line cancelling program was physically measured between the secondary source and the microphone in close proximity to the secondary speaker. The impulse response was then used to obtain the inverse response where both the training impulse response and inverse response FIR filters were set at 40 taps. The system cut-off frequency (anti-aliasing filters) was 7.5 kHz and the sampling frequency 15 kHz. The program was written in *C* and executed on a TI C32 DSP processor.

Fig. 14(a) shows the measured plant impulse response and its inverse. A training delay of 30 samples was required to give good convergence. The inverse, as to be expected, has a large undesirable left handed negative sequence, resembling a second order system with an 'unstable zero' (compare these polarity reversed responses with Fig. 8(c)). Fig. 14(b) shows the modified plant where the left-handed sequence has been considerably reduced. A training delay of only 15 taps is now needed.

Fig. 15 shows the online cancellation using the modified plant function measured in Fig. 14(b), The primary source is represented by a loudspeaker being driven by a signal generator with a

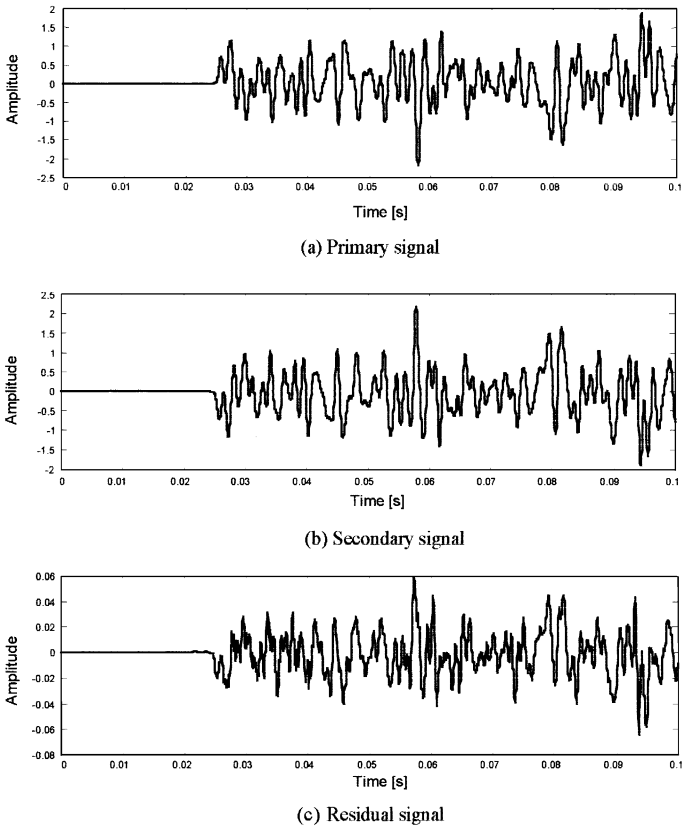

Fig. 13. Cancellation of unpredictable (random) noise. Non-minimum phase plant, cut-off frequency $f_c = 800\,\text{Hz}$, $f_n = 4\,\text{kHz}$.

periodic square wave of periodic frequency 210 Hz. Fig. 15(a) shows the acoustic output from the primary speaker microphone, situated close to the speaker, which provides the input to the computer. It can be seen that the square wave input to the primary speaker is considerably distorted at its acoustic output, modified by the primary speaker response.

Fig. 15(b) shows the output from the computer after the secondary speaker inverse has been applied to the input from the primary microphone. It can be seen that the signal is returned to an approximate square wave again (aided by the fact that the primary and secondary speakers have similar dynamic responses) showing the success of the inverse filtering. Fig. 15(c) shows the acoustic output from the secondary speaker microphone close to the speaker. It shows again a similar distorted output wave from a square wave input signal as the primary speaker (the signal polarity has been reversed for comparison). Fig. 15(d) shows the acoustic output from the error microphone, situated at distance $r_{sm} = 2\,\text{m}$, measuring the net sound from both the primary and secondary speakers. It can be seen that there is almost complete cancellation. All that can be detected is the barometric pressure fluctuations (wind noise). The primary signal can be varied rapidly in frequency and amplitude and the cancelling signal follows, producing small error change, demonstrating the success of the technique.

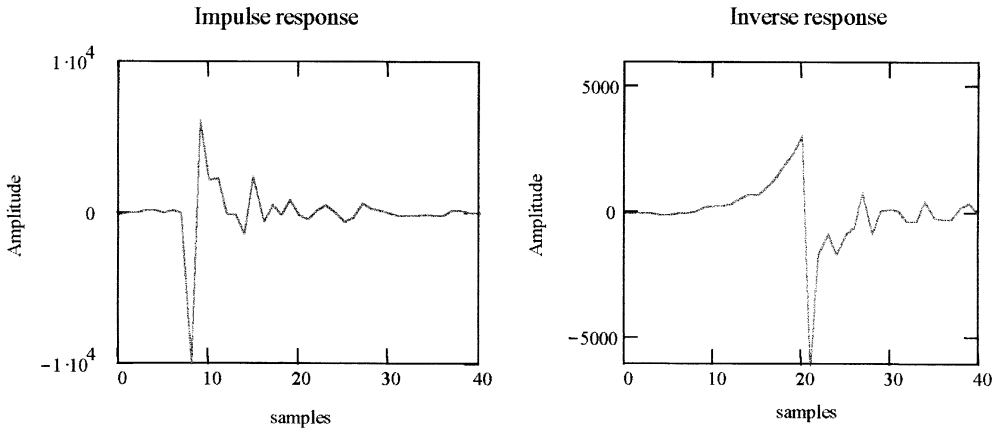

(a) Measured plant responses showing large left hand inverse sequence

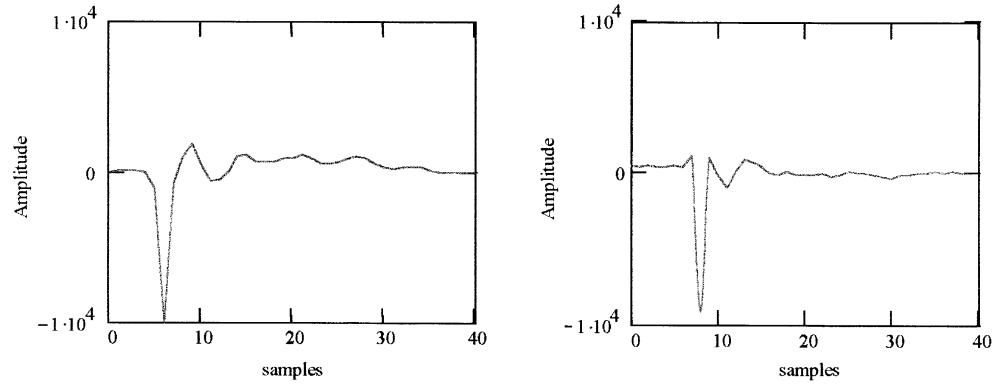

(b) Modified plant responses to minimize the left hand inverse sequence

Fig. 14. Real impulse and inverse plant responses measured with white noise and a 40 tap FIR filter.

4. Conclusions

The paper has considered the development of structures for directional free field ANC cancelling systems. A method to increase the adaptive speed for time varying periodic sources, using conventional adaptive transverse FIR filters, has been described. The method involved dividing the spectrum into bands and applying similar cancelling strengths 'β' in each band. This approach gave approximately equal response irrespective of the frequency amplitude, reducing signal distortion and increasing the overall adaptive speed. Unfortunately, it is found that this method is limited to a finite β, given by the stability band zero bandwidth. This limits the adaptive speed, making the method appropriate for cancelling moderately changing periodic noise but inappropriate for cancelling rapidly changing noise.

To cancel rapidly changing periodic noise and unpredictable statistically non-stationary sources, such as speech and music, an instantaneous cancelling process was described. To succeed,

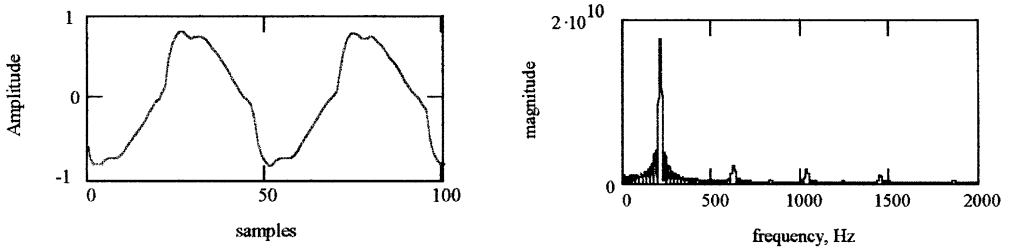

(a) Acoustic output from primary speaker (microphone).

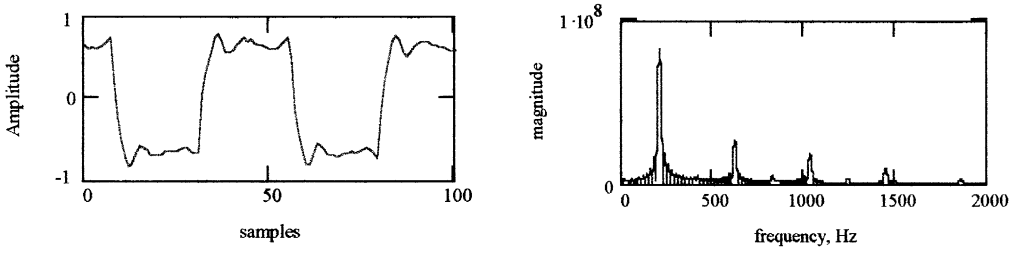

(b) Electrical input (from computer) to secondary speaker.

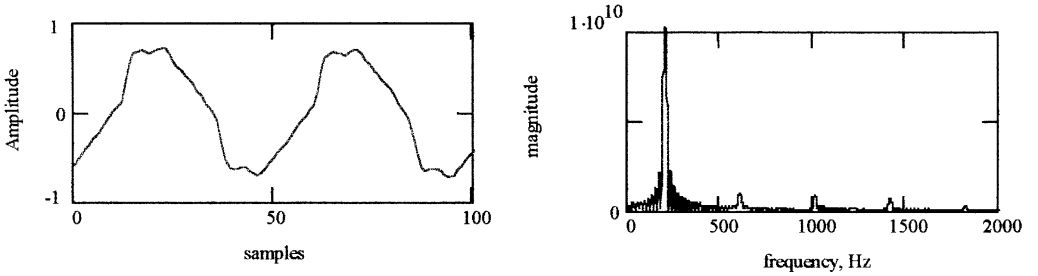

(c) Acoustic output from secondary speaker (microphone).

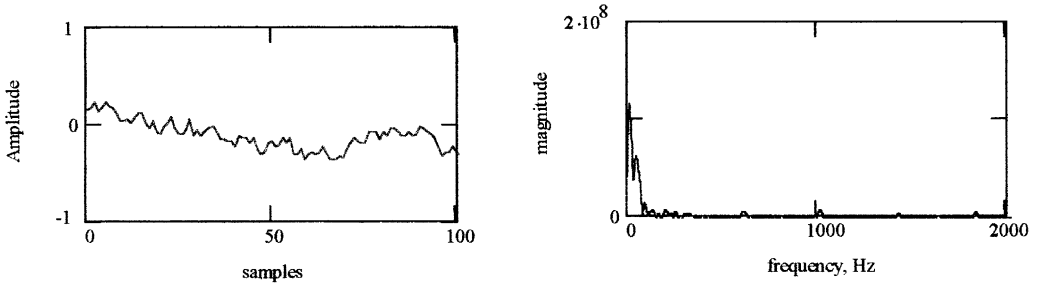

(d) Acoustic output from error microphone at r_{sm}=2m.

Fig. 15. Online cancellation time histories in samples and spectra in Hz for a 210 Hz periodic square wave.

it was found necessary to dispense with the 'slow' on line adaptive FIR filters. A cancelling structure that responded instantaneously, in principle, was to use a negative copy of the primary source signal, compensate for the plant distortion, directly, using its exact inverse and injecting the cancelling signal at the corresponding instantaneity point along the original primary wave. Simulation showed that this approach can give considerable cancellation of the primary source. Implementation of these structures into hardware has given online cancellation that supports the simulation, verifying the viability of the approach. Further detailed investigation of these techniques is ongoing.

Acknowledgements

The authors would like to thank Dragana Nikolic for her computational help in preparing this paper. This work is supported by a DTI SMART award and is protected by Patent Application Number 0208421.8.

References

[1] B. Widrow, J.R. Glover, J.M. McCool, J. Kaunitz, C.S. Williams, R.H. Hearn, J.R. Zeidler, E. Dong, R.C. Goodlin, Adaptive noise canceling: principles and applications, *Proceedings of the IEEE* 63 (12) (1975) 1692–1716.

[2] J.R. Glover, Adaptive noise canceling applied to sinusoidal interference, *IEEE Transactions on Acoustic, Speech, and Signal Processing* ASSP-25 (6) (1977) 484–491.

[3] D.R. Morgan, An analysis of multiple correlation loops with a filter in the auxiliary path, *IEEE Transactions on Acoustic, Speech, and Signal Processing* ASSP-28 (1980) 454–467.

[4] B. Widrow, D. Shur, S. Shaffer, On adaptive inverse control, *Proceedings of the Asilomar Conference*, 1981, pp. 185–189.

[5] G.B.B. Chaplin, R.A. Smith, Waveform synthesis, the Essex solution to repetitive noise and vibration, *Proceedings of the Inter-noise*, 1983, pp. 399–402.

[6] S.J. Elliott, P. Darlington, Adaptive cancellation of periodic synchronously sampled interference, *IEEE Transactions on Acoustic, Speech, and Signal Processing* ASSP-33 (1985) 715–717.

[7] S.J. Elliot, P.A. Nelson, The application of adaptive filtering to the active control of sound and vibration, ISVR Technical Report No. 136, 1985.

[8] P. Darlington, S.J. Elliott, Stability and adaptively controlled systems, a graphical approach, *Proceedings of the ICASSP*, 1987, pp. 399–402.

[9] S.J. Elliott, I.A. Stothers, P.A. Nelson, A multiple error LMS algorithm and its application to the active control of sound and vibration, *IEEE Transactions on Acoustic, Speech, and Signal Processing* ASSP-35 (10) (1987) 1423–1434.

[10] S.E. Wright, B. Vuksanovic, Active control of environmental noise, I, *Journal of Sound and Vibration* 190 (3) (1996) 565–585.

[11] S.E. Wright, B. Vuksanovic, Active control of environmental noise, III: implementation of theory into practice, *Journal of Sound and Vibration* 220 (3) (1999) 469–496.

[12] S.E. Wright, H. Atmoko, Active control of environmental noise, VI: performance of a fundamental free-field cancelling system, *Journal of Sound and Vibration* 245 (4) (2001) 581–609.

[13] S.E. Wright, H. Atmoko, Active control of environmental noise, VII: performance of multi-frequency, multi-channel, free-field sound cancelling systems, *Journal of Sound and Vibration* 258 (2) (2002) 203–232.

[14] S.T. Neely, J.B. Allen, Invertibility of a room impulse response, *Journal of the Acoustic Society of America* 66 (1979) 165–169.

[15] M. Miyoshi, Y. Kaneda, Inverse filtering of room acoustics, *IEEE Transactions on Acoustics, Speech, and Signal Processing* 36 (1988) 145–152.
[16] A. Kaelin, D. von Grunigen, On the use of a priori knowledge in adaptive inverse control, *IEEE Transactions on Circuits and Systems* 47 (1) (2000) 54–62.
[17] B. Widrow, S.D. Stearns, *Adaptive Signal Processing,*, Prentice-Hall, Englewood Cliffs, NJ, 1985.